



---

## **SYNTHESIS AND ELECTRON TRANSPORT PROPERTIES OF SOME NEW 4,7-PHENANTHROLINE DERIVATIVES IN THIN FILMS**

**Cristina M. Al Matarneh<sup>1</sup>, Ramona Danac<sup>1</sup>, Liviu Leontie<sup>2\*</sup>, Florin Tudorache<sup>3</sup>,  
Iulian Petrila<sup>3</sup>, Felicia Iacomi<sup>2</sup>, Aurelian Carlescu<sup>2</sup>, Gigel Nedelcu<sup>2</sup>, Ionel Mangalagiu<sup>1</sup>**

<sup>1</sup>Alexandru Ioan Cuza University of Iasi, Faculty of Chemistry, 11 Carol I Blvd., 700506 Iasi, Romania

<sup>2</sup>Alexandru Ioan Cuza University of Iasi, Faculty of Physics, 11 Carol I Blvd., 700506 Iasi, Romania

<sup>3</sup>Alexandru Ioan Cuza University of Iasi, Interdisciplinary Research Department - RAMTECH,  
11 Carol I Blvd., 700506 Iasi, Romania

---

### **Abstract**

Temperature-dependent d.c. electric conductivity of some recently synthesized organic compounds, 4,7-phenanthroline derivatives is studied. Thin-film samples ( $d=0.34\text{--}0.63\text{ }\mu\text{m}$ ) spin-coated from dimethylformamide solutions onto glass substrates have been used. Organic films with reproducible electron transport properties can be obtained if, after deposition, they are submitted to a heat treatment within temperature range of 298–523K. Examined organic compounds in thin films are polycrystalline and display typical *n*-type semiconductor behavior. The activation energy of d. c. electric conduction ranges between 0.09 and 0.46 eV and is influenced by nature of substituents, degree of conjugation systems and packing capacity of compounds. In the higher temperature range ( $T>433\text{ K}$ ), the electron transport in examined compounds can be interpreted in terms of the band gap representation model, while in the lower temperature range, the Mott's variable-range hopping conduction model was found to be appropriate. Some of the investigated compounds hold promise for thermistor applications.

**Key words:** chemical synthesis, electric conductivity, organic compounds, thin films

*Received: November, 2014; Revised final: February, 2015; Accepted: February, 2015*

---

### **1. Introduction**

Organic semiconductor compounds (in form of monomers, polymers, plastics, synthetic rubbers, etc.) represent an emerging class of materials, extensively explored over the past four decades. The ample worldwide research effort addressed divers aspects, from material synthesis and growth (single crystals, thin films, nanostructures), study of electron transport, optical, and photophysical/photochemical properties, to a wide range of technological applications (Iniewski, 2011; Logothetidis, 2012).

The extended  $\pi$ -electron systems of organic semiconductors can be easily tuned through ‘molecular engineering’ (molecular structure

modification by chemical substitution). In this way, divers classes of emerging materials, ranging from superconducting and semiconducting, to conducting ones have been synthesized to date (Fraxedas, 2006; Lebed, 2008).

Due to their remarkable characteristics, significant electroluminescence, high mobilities of charge carriers, energy band gap in the IR-vis domain, relevant photophysical characteristics, combined with high processability and versatility, easy shaping and manufacture, compatibility with mechanically flexible substrates and facile integration with divers physical/chemical/biological functionalities (Bernards et al., 2008; Huang et al., 2014; Turbiez et al., 2005), organic semiconductors

\* Author to whom all correspondence should be addressed: email: lleontie@uaic.ro

show great promise for a wide range of solid-state device applications, including: transistors, light-emitting diodes, solar cells, sensors, as well as in nanoelectronics, transparent electronics, electro-optics, photonics and spinics (Deleonibus, 2009; Facchetti and Marks, 2010; Kymmissis, 2009; Metzger, 2012; Ohtsu, 2004; Paraschiv 2014; Schols 2011; Sun and Saracftci 2005; Szodrai and Lakatos 2014).

The electron transport properties of organic semiconductor materials employed as active components in semiconductor devices are strongly influenced by their molecular packing, which may significantly affect molecular orbital shapes and interactions (Kazheva et al., 2002). In this respect, study of the structure/property relationship of utilized organic materials becomes extremely important, providing understanding of basic transport mechanisms in these materials and consequently, enabling improvement in the performance of new (opto)electronic devices (Coropceanu et al., 2007; Karl, 2003; Stallinga, 2009; Ueno and Kera, 2008).

In our previous works (Danac, 2014; Leontie et al., 2003a; Leontie et al., 2003b; Leontie et al., 2005a; Leontie et al., 2005b; Leontie et al., 2006; Leontie and Danac, 2006; Leontie, 2007; Leontie, 2009; Leontie, 2010; Leontie, 2011; Leontie, 2012; Prelipceanu, 2007; Rusu et al., 2001; Șunel et al., 1995) electronic transport and optical properties of a

great number of organic compounds showing typical semiconducting behavior have been studied. In this paper, we extend these investigations to some recently synthesized organic compounds, 4,7-phenanthrolin-4-ium salts (SMC compounds), in form of polycrystalline thin films.

## 2. Experimental

## *2.1. Synthesis of compounds*

4-(R-2-oxoethyl)-4,7-phenanthrolin-4-ium bromides have been recently synthesized in our group by a N-alkylation reaction. These salts have been prepared in excellent yields (67-94%) by reaction of 4,7-phenanthroline (**1**) with reactive halides (**2**) in refluxing acetonitrile.

The reaction of N-quaternization of 4,7-phenanthroline undergoes the following transformation (Fig. 1).

The structure of the compounds was proved by elemental and spectral methods (IR, 1H-NMR). They showed good chemical stability under normal ambient atmosphere. Investigated organic compounds correspond to the general formula presented in Fig. 2.

The molecular formulas together with other compounds properties are given in Table 1.

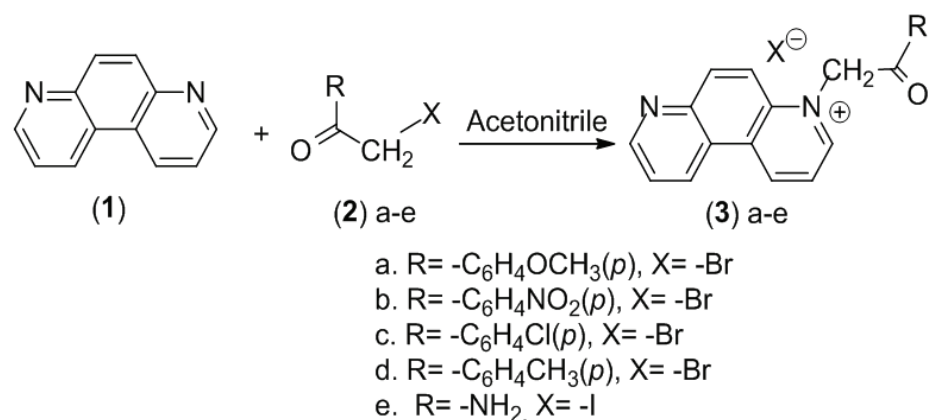
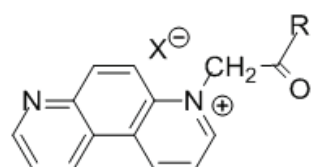


**Fig. 1.** Synthesis pathway of the investigated compounds



- SMC1 (**3a**): 4-(2-(4-methoxyphenyl)-2-oxoethyl)-4,7-phenanthrolin-4-i um bromide  
 SMC2 (**3b**): 4-(2-(4-nitrophenyl)-2-oxoethyl)-4,7-phenanthrolin-4-i um bromide  
 SMC3 (**3c**): 4-(2-(4-chlorophenyl)-2-oxoethyl)-4,7-phenanthrolin-4-i um bromide  
 SMC4 (**3d**): 4-(2-(4-tolyl)-2-oxoethyl)-4,7-phenanthrolin-4-i um bromide  
 SMC5 (**3e**): 4-(2-amino-2-oxoethyl)-4,7-phenanthrolin-4-i um iodide

**Fig. 2.** General structure of the investigated compounds

**Table 1.** Molecular formula and some properties of the investigated compounds

Compound	Molecular formula	Molecular weight, M	Color	Melting point (K)
SMC1	C <sub>21</sub> H <sub>17</sub> BrN <sub>2</sub> O <sub>2</sub>	409.28	beige	526–528
SMC2	C <sub>20</sub> H <sub>14</sub> BrN <sub>3</sub> O <sub>3</sub>	424.25	beige	508–510
SMC3	C <sub>20</sub> H <sub>14</sub> BrClN <sub>2</sub> O	413.69	beige	515–517
SMC4	C <sub>21</sub> H <sub>17</sub> BrN <sub>2</sub> O	393.28	beige	519–521
SMC5	C <sub>14</sub> H <sub>12</sub> IN <sub>3</sub> O	365.17	yellow	537–539

## 2.2. Sample preparation. Electric conductivity measurements

The d. c. electric conductivity of as-synthesized compounds was investigated using thin-film samples [surface-type cells (Căplănuș, 1999–2000; Rusu, 2001; Şunel et al., 1995)] as thin films deposited by sol-gel (spin-coating) technique, at room temperature, onto glass substrates. Dimethylformamide was used as solvent, in which actual compounds SMC1–SMC5 showed good stability. By adjusting the deposition conditions (solution concentration in the range of 3–10 mg/ml, rotation speed by 1500 rot./min, 5–9 coating-drying cycles, respectively, substrate maintained at room temperature, etc), organic films of a constant thickness on large areas of the substrate surface were obtained.

Thin Ag films (about 1 μm thick), thermally evaporated in vacuum (~10<sup>-5</sup> Torr) onto substrates prior to film deposition, served as electrodes; they were separated by a gap of 2–5 mm. In all performed measurements low-intensity electric fields (under 10<sup>2</sup> V·cm<sup>-1</sup>) were applied, so that non-ohmic effects were not noticed.

Thickness (*d*) of thin-film samples was determined with an interferometric microscope MII-4 (LOMO, St. Petersburg) and was found in the range of 0.34–0.63 μm. Surface morphology of organic films was examined by Atomic Force Microscopy (AFM), with a NT-MDT SOLVER PRO-M equipment. The crystal structure of the organic films was investigated by X-ray diffraction (XRD) technique (CuK<sub>α</sub> radiation, wavelength  $\lambda=1.54182 \text{ \AA}$ ), using a DRON-2.0 diffractometer.

The electric conductivity type of the organic thin films under study was determined by thermal-sonde method (Smith, 1980) and was found to be of *n*-type, for all investigated samples. Experimental arrangements used in the study of temperature dependences of d. c. electric conductivity were similar to those presented in (Căplănuș, 1999–2000; Rusu, 2001; Şunel et al., 1995). A KEITHLEY Model 6517B electrometer was used for resistance measurements of organic thin films. Transmission and reflection spectra, in the spectral range of 300–1400 nm, were recorded with a STEAG ETA-Optik spectrometer.

The absorption coefficient of thin-film samples,  $\alpha$ , was determined by using the expression (Pancove, 1979) (Eq. 1), where *d* is the film

thickness and  $I_0$  and  $I$  denote the intensity of incident and emergent beam, respectively.

$$\alpha = \frac{1}{d} \ln\left(\frac{I_0}{I}\right) \quad (1)$$

The above approximate formula (neglecting the effect of reflexion) may be properly used for present organic films, the reflectance of which is below 10 %, for photon energies less than the optical band gap,  $E_{go}$  (Moss, 1994).

## 3. Results and discussion

As revealed by the XRD study (Fig. 3), examined organic thin films exhibit a prevailing polycrystalline structure, with a high degree of crystallinity. Structural investigations showed that sample structure depend on the compound nature (molecular structure), thin-film thickness (increased film thickness generally leading to larger grain sizes), and deposition conditions.

All examined samples were found to display the most preferred planes parallel to substrate surface. The interplanar spacings ( $d_{hkl}$ ) of studied organic samples were calculated by using the Bragg equation (Cullity and Stock, 2001; Pecharsky and Zavalij, 2009) (Eq. 2), where  $\theta$  denotes the Bragg diffraction angle,  $\lambda=1.54182 \text{ \AA}$  is the wavelength of the incident X-ray beam and *n* is the reflection order; *h*, *k*, *l* are Miller indices, used to express crystal lattice planes and directions.

$$2d_{hkl} \sin \theta = n\lambda \quad (2)$$

The average crystallite size (*D*) was determined by means of Debye-Scherrer equation, supposing a negligible residual strain effect (Cullity and Stock, 2001; Pecharsky and Zavalij, 2009) (Eq. 3), where  $k=0.9$  (Cullity and Stock, 2001) denotes the Scherrer constant,  $\lambda=1.54182 \text{ \AA}$  is the X-ray wavelength,  $\beta$  is the angular full-width at half-maximum (FWHM) of the XRD peak in radians, and  $\theta$  is the Bragg diffraction angle corresponding to respective peak.

$$D = \frac{k\lambda}{\beta \cos \theta} \quad (3)$$

Values of some typical parameters, determined according to standard method for structural analysis (Cullity and Stock, 2001), are

given in Table 2. As can be observed from this table, investigated organic thin films display rather small crystallites, the size of which is ranged between 15.75 and 60.58 nm. The polycrystalline structure, which is prevalent in the case of actual organic films, exerts a strong influence on the electron transfer mechanism in examined samples: additional scattering produced by film surfaces and small crystallite boundaries tends to substantially diminish the charge carrier mobilities and electric conductivity, with respect to those of the bulk materials (Kazmerski, 1980). The AFM study of organic thin-film samples revealed (Fig. 4) a preponderant grain-like surface morphology, as characteristic topographical feature. Actual organic films display a typical polycrystalline, compact and pinhole-free microstructure; they contain grains of different shapes and sizes, the basis of which lays on the film surface. As resulted from the analysis of AFM micrographs for different organic samples, the mean values of the root mean square (RMS) roughness laid in the range of 6.8–48.3 nm, while the mean grain sizes ranged between 20 and 52 nm.

In our previous works, above-mentioned, we have studied the electron transport properties of many classes of heterocyclic compounds (in polycrystalline thin films, deposited from solution) with similar molecular conformations, which were found to exhibit typical semiconductor properties.

It was experimentally established that organic thin-film samples with stable solid-state structure and reproducible electron transport properties (reversible temperature dependences of electric conductivity, Seebeck coefficient etc.) can be obtained if they are submitted to a heat treatment consisting of several successive heating and cooling cycles within a certain temperature interval,  $\Delta T$ , characteristic to each compound (Table 3).

The above statement was confirmed by actual experiments. Analysis of temperature ( $T$ ) dependence of d. c. electric conductivity ( $\sigma$ ) for thin organic films with different thickness may provide valuable information on the processes taking place during the heat treatment (Danac, 2014; Leontie et al., 2005a; Rusu, 2001; Sunel et al., 1995).

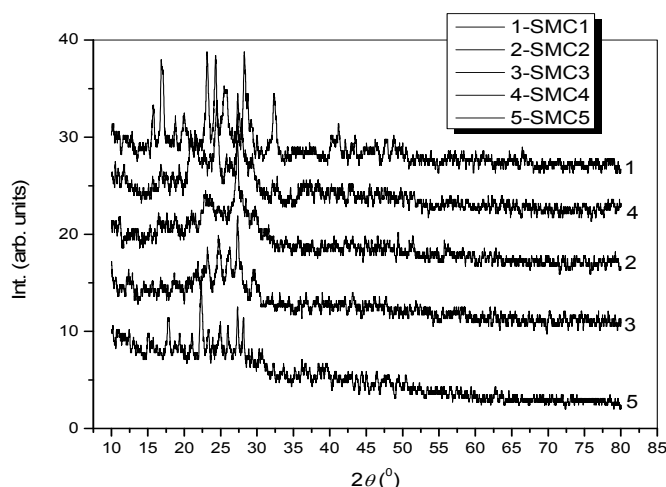


**Fig. 3.** XRD patterns of examined organic compounds

**Table 2.** Typical crystallite size values for SMC compounds

Compound	D ( $\mu\text{m}$ )	2θ (°)	$d_{hkl}$ (nm)	D (nm)
SMC1	0.39	16.85	0.0916	19.53
		23.12	0.0912	24.23
		24.31	0.1928	27.41
		28.26	0.0771	23.8
SMC2	0.44	27.32	0.0868	18.59
SMC3	0.48	23.2	0.0937	60.58
		24.7	0.3591	15.75
		26.25	0.1454	20.81
		27.35	0.0861	18.59
SMC4	0.40	24.45	0.2303	17.71
		27.36	0.0859	29.48
SMC5	0.46	17.79	0.1526	21.56
		22.33	0.0782	23.52
		24.97	0.94845	27.45
		25.99	0.1855	31.58
		27.31	0.0870	32.88
		28.12	0.0773	38.93

d-thin-film thickness; θ-Bragg angle;  $d_{hkl}$ -interplanar spacing for a family of atomic planes with (hkl) Miller indices; D-crystallite size

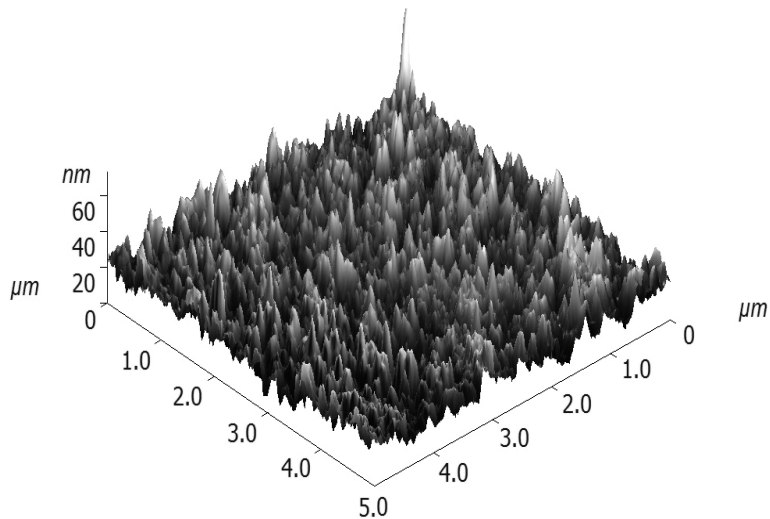


**Fig. 4.** Typical AFM image for thin-film organic samples: compound SMC4 (RMS=6.85 nm)

Actual experiments indicate that the shapes of the electric conductivity-temperature dependences are similar to those presented and discussed in (Danac, 2014; Leontie et al., 2005b; Leontie, 2011; Rusu, 2001; Sunel et al., 1995).

The electric conductivity of all examined samples was found to increase together with temperature over the whole range investigated. For a large number of organic compounds with similar molecular structures, we found that the well-known exponential law (Meier, 1974; Seeger, 1999) (Eq. 4), can suitable describe the experimental electric conductivity-temperature dependences, where  $E_a$  is the thermal activation energy of electric conduction,  $\sigma_0$  denotes a characteristic parameter depending on the compound nature and  $k_B$  is the Boltzmann's constant.

$$\sigma = \sigma_0 \exp\left(-\frac{E_a}{k_B T}\right) \quad (4)$$

According to the band model representation, in the intrinsic conduction domain (for  $T > T_c$ , where  $T_c$  is a characteristic temperature, given in Table 3), the thermal activation energy is equal to half of the forbidden bandwidth of the material,  $E_g$  ( $E_a = E_g/2$ ), which coincides with the energy difference between conduction band (CB) minimum and the valence band (VB) top. Besides, within the extrinsic conduction domain ( $T < T_c$ ), it indicates the energy of donor levels measured with respect to the bottom of CB, or that of the acceptor levels with respect to the VB maximum, for *n*-type or *p*-type conduction, respectively (Gutman and Lyons, 1981; Kazmerski, 1980; Meier, 1974; Seeger, 1999).

According to Eq. (4), the experimental  $\ln\sigma=f(10^3/T)$  plots must be linear, under the assumption of a temperature-independent preexponential factor. We supposed that for examined organic films an exponential temperature

dependence of d. c. electric conductivity, described by law (4), is also possible; consequently, we have examined the shape of  $\ln\sigma=f(10^3/T)$  dependences during the heat treatment. The obtained curves, depending on the compound nature, thin-film sample thickness and preparation conditions for organic films, also display some similar trends for all investigated samples. Fig. 5 illustrates a typical experimental  $\ln\sigma=f(10^3/T)$  dependence during the heat treatment for one of the organic compounds, subjected to three successive heating/cooling cycles. Some modifications in thin-film microstructure (grain size and shape, characteristics of intergrain boundaries, etc.) and purity (by removal of the adsorbed/absorbed gases, as well as of some accidental impurities) (Danac, 2012; Leontie, 2012; Rusu, 2007) may occur, especially, during the first heating run (Fig. 5).

Our experiments showed that after 2–3 series of successive heating/cooling cycles, the temperature dependences of electric conductivity become reversible. This behavior denotes stabilization of thin-film solid-state structure within the investigated temperature range (Danac, 2012; Rusu et al., 2001).

As can be ascertain from Figs. 4 and 5, the obtained  $\ln\sigma=f(10^3/T)$  curves of heat-treated organic thin-film samples are typical for wide band gap semiconductors. They generally exhibit a portion with a smaller slope, within the lower temperature range ( $T < T_c$ ), and a portion with a larger slope in the higher temperature domain ( $T > T_c$ ). The two different slopes denote different activation energies and different conduction mechanisms operating in present organic films in indicated temperature ranges. In the lower temperature region, the organic films display a prevailing extrinsic conductivity. For this temperature range, the slope of the  $\ln\sigma=f(10^3/T)$  curves corresponds to the energy of the donor levels, measured with respect to the CB minimum (since actual organic films exhibit a predominant *n*-type conduction). The values of the thermal activation

energy in the low temperature range ( $E_{a1}$ ) lay between 0.09 and 0.14 eV (Table 3).

Several models have been proposed to explain the electric conduction mechanisms in organic semiconducting thin films. According to the crystallite boundary trapping theory (Baccarani et al., 1978; Leontie and Rusu, 2006), a high density of trap states occurs at the crystallite boundary, which favors capture of the free carriers. So created space charge causes a bending of the energy bands and occurring of potential barriers (usually rather low, under 0.1 eV). These barriers determine a decrease in electric conductivity of polycrystalline samples.

We consider that obtained values for the activation energy in the low temperature range ( $E_{a1}$ ) are unusually high to use mentioned conduction models, based on grain barrier-limited electron transport. Besides, taking into account the structural features of actual samples, we consider that crystallite boundary trapping models are not applicable to actual organic films, instead the hopping conduction mechanism could be more appropriate for the lower temperature range.

In the higher temperature range, an intrinsic conduction mechanism operates in studied organic films. As our experiments revealed, the intrinsic conduction domain begins at a certain temperature,  $T_c$  (Table 3), which depends on the compound nature and organic thin-film thickness. During the heat treatment,  $T_c$  values were found shift to the lower temperature range; this behavior indicates a diminution of the impurity and structural defect density in organic films under study (Leontie et al., 2005a; Leontie et al., 2005b; Rusu, 2001).

The values of activation energy for the higher temperature range were found to depend on the compound nature.

As can be inferred from Fig. 5, the slopes of experimental  $\ln\sigma=f(10^3/T)$  curves don't change during heat treatment within  $T>T_c$  range. Besides, the shape of conductivity-temperature curves registered for a given compound, prepared with different solvents, exhibited certain changes in the lower temperature range, but not in the higher temperature domain. Also, for a series of organic compounds,  $E_a$  values, determined from the optical absorption spectra, were found to be close to values obtained from electric measurements (Rusu, 2007). These features confirm that in the respective temperature intervals an intrinsic conduction mechanism does operate. Consequently, we have determined the values of the thermal activation energy for the investigated organic thin films, from the slope of the experimental  $\ln\sigma=f(10^3/T)$  curves, within the intrinsic conduction domain, according to Eq. (4) and listed them in Table 3 ( $E_{a2}$ ). The experimental temperature dependences of electric conductivity (Figs. 5 and 6) suggest that in the higher temperature range ( $T>T_c$ ), the band model representation could be applied for the study of electron transport mechanism in present organic thin-film samples.

Analysis of the d. c. electric conductivity data reveals that the organic compounds under study exhibit a typical *n*-type semiconductor-like behavior, which is determined by the thin-film structure (predominantly polycrystalline), as well as specific molecular configurations.

**Table 3.** Temperature dependence of the electric conductivity for SMC compounds

Compound	d (μm)	ΔT <sub>1</sub> (K)	E <sub>a1</sub> (eV)	ΔT <sub>2</sub> (K)	ΔT (K)	T <sub>c</sub> (K)	E <sub>a2</sub> (eV)
SMC1	0.39	298–343	0.14	433–508	298–508	442	0.41
SMC2	0.44	298–353	0.10	423–493	298–493	433	0.41
SMC3	0.48	298–353	0.09	433–498	298–498	434	0.39
SMC4	0.40	298–343	0.12	363–498	298–498	432	0.36
SMC5	0.46	298–363	0.13	453–523	298–523	483	0.46

*d*-film thickness; ΔT<sub>1</sub>, ΔT<sub>2</sub>: temperature ranges for extrinsic and intrinsic conduction domains, respectively; E<sub>a1</sub>, E<sub>a2</sub>-thermal activation energies of electric conduction within temperature ranges ΔT<sub>1</sub> and ΔT<sub>2</sub>, respectively; ΔT-whole temperature range for the heat treatment; T<sub>c</sub>-characteristic temperature (for T>T<sub>c</sub>, conductivity of heat treated samples become intrinsic); E<sub>a2</sub>-thermal activation energy of electric conduction after the heat treatment.

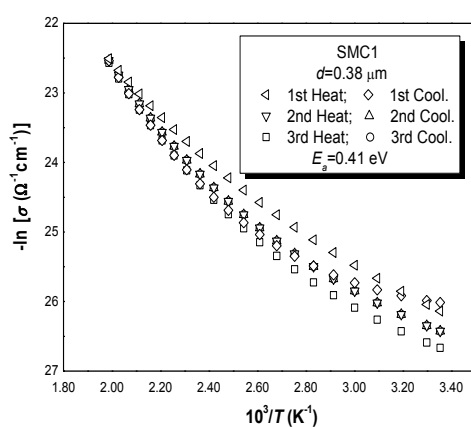


**Fig. 5.** Temperature dependence of electric conductivity during the heat treatment: compound SMC1

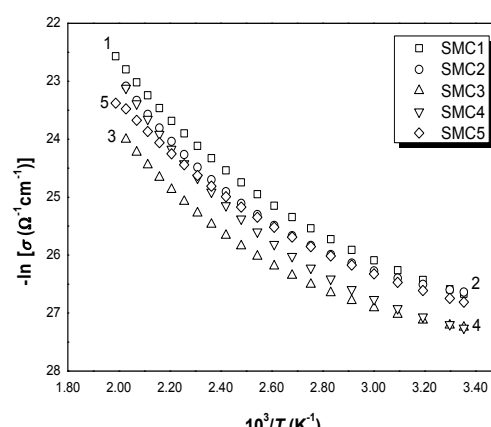


**Fig. 6.** Temperature dependence of electric conductivity for the heat-treated samples (SMC series)

The examined organic semiconductor materials exhibit extended conjugation systems, which facilitate the electron transfer and serve to the enhancement of the d. c. electric conduction at the intramolecular level. The degree of conjugation can be substantially influenced by the nature and position of the substituents (R) within the organic molecule (Danac, 2012, 2014; Leontie, 2012; Rusu, 2007), which affect the obtained values of the activation energy ( $E_a$ , Table 3). These values were found to be smaller for extended conjugation systems.

On the other hand, intermolecular d. c. conduction processes, significantly influenced by intermolecular arrangement, need to be taken into consideration. The small-molecule polycrystalline organic semiconductors contain closed-shell molecular moieties, which are bound to each other by weak Van der Waals forces. The strong coupling between  $\pi$ -electrons of overlapping molecules in present compounds results in an enhanced carrier delocalization, which constitutes another important factor strongly affecting the electric conduction mechanism at the intermolecular level, in these materials. Therefore, molecular packing plays a key role in electron transport behavior of small-molecule organic compounds in polycrystalline thin films (Horowitz, 1998).

The registered differences between obtained thermal activation energies of five investigated compounds can be explained considering both their capacity to enable extended planar conjugation systems and the significant capability of compact packing in overlapping monomolecular layers.

The skeleton of the investigated compounds is the aromatic planar 4,7-phenanthroline heterocycle, possessing a strong and extended conjugation of its  $\pi$ -electrons. This main part of the molecule remains unchanged in the investigated compounds, thus the differences between the values of thermal activation energy of electrical conduction are small. Packing in overlapping molecular layers is enhanced in the case of compounds showing less voluminous phenyl substituents. Thus compound SMC4, having a small methyl group as substituent on the phenyl ring, shows the lowest value of the activation energy of electric conduction. Larger volume substituents may cause steric perturbation of their local environments, leading to a decreased packing capacity.

It is known that in the case of polycrystalline films, the electron transport properties of which are strongly influenced by inter-grain characteristics, determination of the energy band gap from absorption spectra is more appropriate (Harbecke, 1985; Greenaway, 1968). In the region of the fundamental absorption threshold, the absorption coefficient,  $\alpha$ , depends on the energy of the incident photon,  $h\nu$ , according to the relation (5) (Pancove, 1979) where:  $n=1/2$  and 2 for optical direct and indirect allowed transitions, respectively,  $E_{go}$  is the optical band gap, direct ( $E_{go}^d$ ) or indirect, and  $A$  is a

characteristic parameter which is independent on the photon energy.

$$\alpha h\nu = A(h\nu - E_{go})^n \quad (5)$$

According to the above equation, low energy portions of  $\alpha h\nu=f(h\nu)$  curves can be fitted to any of standard dependences, in particular  $(\alpha h\nu)^2=f(h\nu)$  for allowed direct transitions. The analysis of actual experimental data (Fig. 7) shows that the best fitting is obtained for  $(\alpha h\nu)^2=f(h\nu)$  dependences and consequently, these curves have been used for estimation of the optical band gap values, by extrapolating respective straight lines to  $\alpha h\nu \rightarrow 0$ . Obtained values are listed in Table 4.

The experimental data indicate that the examined compounds have direct band gaps ( $E_{go}^d$ ) ranging between 3.82 and 4.33 eV. The obtained values (Table 4) are greater with respect to the  $2E_a$  values (Table 3). This fact is due to the quite different nature of the carrier excitation in the respective processes (optical absorption and electric conduction). The values of  $E_{go}^d$  correspond to band-to-band transitions, whereas those of the  $E_a$  are determined by the electronic transport mechanism in present organic films (Leontie, 2011).

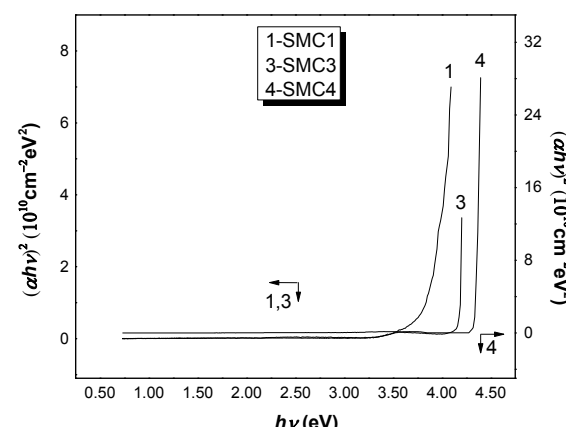


Fig. 7. Optical absorption of investigated organic films

We assumed that in the lower temperature range ( $T < T_c$ ), the Mott's variable-range hopping (VRH) model (Mott and Davis, 1979; Mott et al., 1975; Pope and Swenberg, 1999; Shklovskii and Efros, 1984) may be used to adequately explain the temperature dependence of d. c. electric conductivity of the actual organic films. According to the VRH model, for three-dimensional systems, the conductivity-temperature dependence can be described by (Mott et al., 1975; Pope and Swenberg, 1999; Shklovskii and Efros, 1984) (Eqs. 6, 7).

$$\sigma = \sigma_0 \cdot \exp \left[ -\left( T_0 / T \right)^{1/4} \right] \quad (6)$$

where:

$$\sigma_0 = e^2 R^2 \nu_0 N(E_F) \quad (7)$$

is a pre-exponential factor and  $R$  is the hopping distance, expressed as Eq. (8).

$$R^2 = [9/8\pi\alpha k_B N(E_F)]^{1/4} T^{1/2} \quad (8)$$

The parameter  $T_0$  is a characteristic Mott temperature, characterizing the degree of disorder (Mott and Davis, 1979) (Eq. 9).

$$T_0 = \frac{\lambda \alpha^3}{k_B N(E_F)} \quad (9)$$

In the above relationships  $N(E_F)$  represents the density of the localized states at the Fermi level  $E_F$ ,  $\alpha^{-1}$  ( $\alpha=10^7$  cm $^{-1}$ ) is the coefficient of exponential decay for a localized state wave function near Fermi level,  $\lambda$  denotes a dimensionless constant [of about 18 (Rusu et al., 2007)],  $\nu_0$  is the typical phonon frequency,  $e$  is electron charge, and  $k_B$  is the Boltzmann's constant. The parameter  $\sigma_0$  can be expressed in the form of Eq. (10). (Mott et al., 1975).

$$\sigma_0 = \sigma^* T^{-1/2} \quad (10)$$

$\sigma^*$  is a new pre-exponential factor and Eq. (6) may be written as Eq. (11), where  $\sigma^*$  and  $T_0$  represent the Mott's characteristic parameters.

$$\sigma = \sigma^* T^{-1/2} \cdot \exp[-(T_0/T)^{1/4}] \quad (11)$$

Assuming that  $\sigma_0$  is not depending on temperature, in virtue of Eq. (6) the  $\ln(\sigma T^{1/2})=f(T^{1/4})$  curves have to be linear. For the organic compounds under study, these dependences, in the lower temperature range,  $298 \text{ K} < T < T_c$ , are presented in Fig. 8. As can be observed from the last figure, the obtained experimental dependences are linear, which indicates the validity of the VRH model in adequately explaining the temperature dependence of d. c. electric conductivity of actual organic compounds in thin films, in the lower temperature range.

By using data from Fig. 8 in Eq (11), the values of the Mott's parameters  $\sigma^*$  and  $T_0$  have been calculated and listed in Table 5. We also checked suitability of investigated compounds for potential thermistor applications.

The working of a thermistor is essentially based on the temperature dependence of the electric resistance of a semiconductor material, within the intrinsic conduction regime, that can be described by Eq. (12), where  $R_T$  is the electric resistance at temperature  $T$ ,  $R_\infty$  represents a parameter depending on the compound nature, and  $B$  characterizes the temperature sensitivity of the thermistor.

$$R_T = R_\infty \cdot \exp\left(\frac{B}{T}\right) \quad (12)$$

The temperature coefficient of the resistance, defined by Eq. (13)

$$\alpha_T = \frac{1}{R} \frac{dR}{dT} \quad (13)$$

can be expressed as a function of temperature, by means of Eq. (12) (Eq. 14).

$$\alpha_T = -\frac{B}{T^2} \quad (14)$$

The obtained values of the characteristic parameters  $\alpha_T$  (at temperature  $T=473$  K) and  $B$  are listed in Table 6 for the examined organic films. It can be concluded that some of the compounds under study can be recommended for use as thermistor materials.

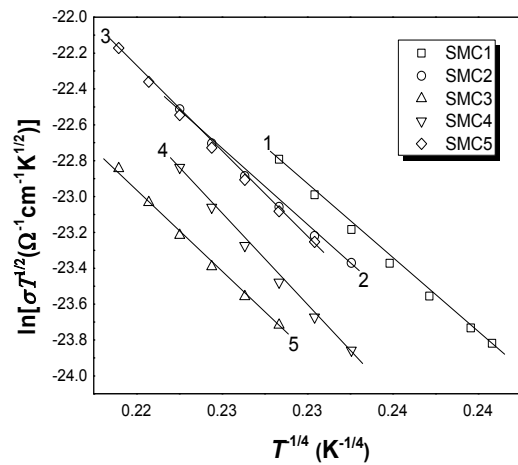


Fig. 8. Mott's variable-range hopping (VRH) conduction (lower temperature range,  $298 \text{ K} < T < T_c$ ) in the heat-treated samples

Table 4. Typical results of optical measurements

Sample	d (nm)	$E_{go}^d$ (eV)
SMC1	389	3.82
SMC3	478	4.18
SMC4	403	4.33

$E_{go}^d$ -direct optical energy band gap

**Table 5.** Mott parameters,  $\sigma^*$  and  $T_0$ , for five samples under study

Compound	$d$ ( $\mu\text{m}$ )	$\Delta T$ (K)	$T_0$ (K)	$\sigma^*$ ( $\Omega^{-1} \cdot \text{cm}^{-1} \cdot \text{K}^{1/2}$ ) (at 353 K)
SMC1	0.38	298–353	$1.10 \times 10^8$	$2.27 \times 10^0$
SMC2	0.44	333–383	$1.28 \times 10^8$	$4.61 \times 10^0$
SMC3	0.47	353–403	$1.82 \times 10^8$	$2.17 \times 10^1$
SMC4	0.40	333–383	$2.57 \times 10^8$	$3.14 \times 10^2$
SMC5	0.45	343–403	$1.92 \times 10^8$	$6.03 \times 10^1$

$\Delta T$ -low temperature investigated temperature range

**Table 6.** Characteristic thermistor parameters of investigated compounds

Compound	$D$ ( $\mu\text{m}$ )	$-a$ ( $\text{K}^1$ ) <sup>a</sup>	$B$ (K)
SMC1	0.38	0.013	2970
SMC2	0.44	0.011	2640
SMC3	0.47	0.010	2410
SMC4	0.40	0.013	3080
SMC5	0.45	0.012	2750

<sup>a</sup> For  $T=473$  K

#### 4. Conclusions

The recently synthesized organic compounds, 4,7-phenanthroline-4-ium salts (SMC compounds) in thin films, behave as typical *n*-type polycrystalline semiconductors.

The electron transfer in the investigated compounds is strongly influenced by their specific molecular structures, enabling formation of extended conjugation systems, as well as their packing capacity.

In the higher temperature range ( $T > T_c$ ), the d.c. electric conductivity of examined compounds can be described in terms of the band gap representation model. In the lower temperature domain (298 K  $< T < T_c$ ) the Mott's variable-range hopping model can be conveniently used.

#### Acknowledgements

This work was supported by the ANCS (National Authority for Scientific Research), Ministry of Economy, Trade and Business Environment, through the National Program Capacities, Project No. 257/28.09.2010 (Acronym CERNESIM), European Social Found, Sectorial Operational Program Human Resources Development 2007–2013, through the strategic grant POSDRU/159/1.5/S/137750, project "Doctoral and Postdoctoral programs support for increased competitiveness in Exact Science research".

#### References

- Baccarani G., Riccò B., Spandini G.J., (1978), Transport properties of polycrystalline silicon films, *Journal of Applied Physics*, **49**, 5565-5570.
- Bernards D.A., Owens R.M., Malliaras G.G., (2008), *Organic Semiconductors in Sensor Applications* (Springer Series in Material Science), Springer-Verlag, Berlin-Heidelberg.
- Căpălănuș I., (1999-2000), On the electrical properties of some purified enzymes in thin films, *Scientific Annals of Al. I. Cuza University of Iasi (Physics)*, **XLV-XLVI**, 224–228.
- Coropceanu V., Cornil J., da Silva Filho D. A., Olivier Y., Silbey R., Brédas J.-L., (2007), Charge transport in organic semiconductors, *Chemistry Review*, **107**, 926-952.
- Cullity B.D., Stock R.S., (2001), *Elements of X-Ray Diffraction*, 3<sup>rd</sup> Edition, Prentice Hall, New Jersey.
- Danac R., Leontie L., Carlescu A., Rusu G.I., (2012), DC electric conduction mechanism of some newly synthesized indolizine derivatives in thin films, *Materials Chemistry and Physics*, **134**, 1042-1048.
- Danac R., Leontie L., Girtan M., Prelipceanu M., Graur A., Carlescu A., Rusu G. I., (2014), On the direct current electric conductivity and conduction mechanism of some stable disubstituted 4-(4-pyridyl)pyridiniumylides in thin films, *Thin Solid Films*, **556**, 216-222.
- Deleonibus S., (2009), *Electronic Device Architectures for the Nano-CMOS Era: From Ultimate CMOS Scaling to Beyond CMOS Devices*, Pan Stanford Publishing, Singapore.
- Facchetti A., Marks T.J., (2010), *Transparent Electronics: From Synthesis to Applications*, Wiley, Chichester.
- Fraxedas J., (2006), *Molecular Organic Materials. From Molecules to Crystalline Solids*, Cambridge University Press, Cambridge-New York-Melbourne-Madrid-Cape Town-Singapore-São Paulo.
- Greenaway D. L., Harbeck G., (1968), *Optical Properties and Band Structure of Semiconductors*, Pergamon, Oxford.
- Gutman F., Lyons L.E., (1981), *Organic Semiconductors, Part A*, Robert E. Publishing, Malabar, Fl.
- Harbeck G., (1985), *Polycrystalline Semiconductors: Physical Properties and Applications*, Springer, Berlin.
- Horowitz G., (1998), Organic field-effect transistors, *Advanced Materials*, **10**, 365-377.
- Huang Y., Tian Y., Cheng W., (2014), Optimization of energy saving for wireless sensor networks, *Environmental Engineering and Management Journal*, **13**, 1057-1070.
- Iniewski K., (2011), *Nanoelectronics-Nanowires, Molecular Electronics, and Nanodevices*, McGraw Hill, New York.
- Karl N., (2003), Charge carrier transport in organic semiconductors, *Synthetic Metals* **133-134**, 649-657.

- Kazheva O.N., Kushch N.D., Aleksandrov G.G., Dyachenko O.A., (2002), Crystal structure and molecular packing in a new organic semiconductor-penta[bis(ethylenedithio)tetrathiafulvalene]-hexathiocyanatomononitratoyttrium(III)-ethanol, *Materials Chemistry and Physics*, **73**, 193-197.
- Kazmerski L.L., (1980), *Polymer and Amorphous Thin Films and Devices*, Academic, New York.
- Kymissis I., (2009), *Organic Field Effect Transistors: Theory, Fabrication and Characterization*, Springer-Verlag, New York.
- Lebed A.G., (2008), *The Physics of Organic Superconductors and Conductors*, Springer Series in Materials Science, Vol. 110, Springer-Verlag, Berlin-Heidelberg-New York.
- Leontie L., Druta I., Alupoae R., Rusu G. I., (2003a), On the electronic transport in some new synthesized high resistivity organic semiconductors in thin films, *Materials Science and Engineering B*, **100**, 252-258.
- Leontie L., Roman M., Brinza F., Podaru C., Rusu G. I., (2003b), Electrical and optical properties of some new synthesized ylides in thin films, *Synthetic Metals*, **138**, 157-163.
- Leontie L., Druta I., Danac R., Prelipceanu M., Rusu G.I., (2005a), Electrical properties of some new high resistivity organic semiconductors in thin films, *Progress in Organic Coatings*, **54**, 175-181.
- Leontie L., Druta I., Danac R., Rusu G.I., (2005b), On the electronic transport properties of pyrrolo[1,2-a][1,10]phenanthroline derivatives in thin films, *Synthetic Metals*, **155**, 138-145.
- Leontie L., Danac R., (2006), Optical properties of some new synthesized organic semiconductors in thin films, *Scripta Materialia*, **54**, 175-179.
- Leontie L., Rusu G. I., (2006), On the electronic transport properties of bismuth oxide thin films, *Journal of Non-Crystalline Solids*, **352**, 1475-1478.
- Leontie L., Druta I., Danac R., (2006), Electrical conduction mechanism in N-(p-R-phenacyl)-4,5-diazafluorenium-9-one bromides thin films, *Synthetic Metals*, **156**, 224-229.
- Leontie L., Druta I., Furdui B., Rusu G. I., (2007), On the mechanism of electrical conduction in some new quaternary salts of bipyridine and indolizine pyridine in thin films, *Progress in Organic Coatings*, **58**, 303-311.
- Leontie L., Druta I., Rotaru Al., Apetroaei N., Rusu G. I., (2009), Electronic transport properties of some new monoquaternary salts of 4,4'-bipyridine in thin films, *Synthetic Metals*, **159**, 642-648.
- Leontie L., Danac R., Druta v., Carlescu A., Rusu G.I., (2010), Newly synthesized fused heterocyclic compounds in thin films with semiconductor properties, *Synthetic Metals*, **160**, 1273-1279.
- Leontie L., Danac R., Apetroaei N., Rusu G.I., (2011), Study of electronic transport properties of some new N-(p-R-phenacyl)-1,7-phenanthrolinium bromides in thin films, *Materials Chemistry and Physics*, **127**, 471-478.
- Leontie L., Danac R., Girtan M., Carlescu A., Rambu A. P., Rusu G. I., (2012), Electron transport properties of some new 4-tert-butylcalix[4]arene derivatives in thin films, *Materials Chemistry and Physics*, **135**, 123-129.
- Logothetidis S., (2012), *Nanostructured Materials and Their Applications*, Springer-Verlag, Berlin, Heidelberg.
- Meier H., (1974), *Organic Semiconductors*, Verlag Chemie, Weinheim.
- Metzger R.M., (2012), *Unimolecular and Supramolecular Electronics I: Chemistry and Physics Meet at Metal-Molecule Interfaces*, Springer, Heidelberg-Dordrecht-London-New York.
- Moss T.S., Balkanski M., (1994), *Handbook on Semiconductors, Optical Properties of Semiconductors*, North-Holland, Elsevier, Amsterdam.
- Mott N.F., Davis E.A., Street R.A., (1975), States in the gap and recombination in amorphous semiconductors, *Philosophia Magna*, **32**, 961-996.
- Mott N.F., Davis E.A., (1979), *Electron Processes in Non-Crystalline Materials*, Clarendon, Oxford.
- Ohtsu M., (2004), *Progress in Nano-electro Optics III*, Springer-Verlag, Berlin-Heidelberg.
- Pancove J., (1979), *Optical Processes in Semiconductors*, Prentice-Hall, Englewood Cliffs, NJ.
- Paraschiv L.S., Paraschiv S., Ion I.V., (2014), Experimental and theoretical analyses on thermal performance of a solar air collector, *Environmental Engineering and Management Journal*, **13**, 1965-1970.
- Pecharsky V.K., Zavalij P.Y., (2009), *Fundamentals of Powder Diffraction and Structural Characterization of Materials*, 2<sup>nd</sup> Edition, Springer, New York.
- Pope M., Swenberg C.E., (1999), *Electronic Processes in Organic Crystals and Polymers*, 2<sup>nd</sup> Edition, Oxford University Press, New York-Oxford.
- Prelipceanu M., Prelipceanu O.S., Leontie L., Danac R., (2007), Photoelectron spectroscopy investigations of pyrrolo[1,2-a][1,10]phenanthroline derivatives, *Physics Letters A*, **368**, 331-335.
- Rusu G.I., Căplănuș I., Leontie L., Airinei A., Butuc E., Mardare D., Rusu I.I., (2001), Studies on the electronic transport properties of some aromatic polysulfones in thin films, *Acta Materialia*, **49**, 553-559.
- Rusu G.I., Airinei A., Rusu M., Prepelită P., Marin L., Cozan V., Rusu I.I., (2007), On the electronic transport mechanism in thin films of some new poly(azomethine sulfone)s, *Acta Materialia*, **55**, 433-442.
- Schols S., (2011), *Device Architecture and Materials for Organic Light-Emitting Devices: Targeting High Current Densities and Control of the Triplet Concentration*, Springer-Verlag, Dordrecht-Heidelberg-London-New York.
- Seeger K., (1999), *Semiconductor Physics*, Springer-Verlag, Berlin-Heidelberg-New York.
- Shklovskii B. I., Efros A. L., (1984), *Electronic Properties of Doped Semiconductors*, Springer-Verlag, Berlin.
- Smith R., (1980), *Semiconductors*, Cambridge University Press, London.
- Stallinga P., (2009), *Electrical Characterization of Organic Electronic Materials and Devices*, Wiley, Chichester.
- Sun S.-S., Saracftci N.S., (2005), *Organic Photovoltaics: Mechanisms, Materials, and Devices*, CRC Press, Taylor & Francis, Boca Raton-London-New York-Singapore.
- Szodrai F., Lakatos Á., (2014), Measurements of the thermal conductivities of some commonly used insulating materials after wetting, *Environmental Engineering and Management Journal*, **13**, 2881-2886.
- Şunel V., Rusu G. I., Rusu G. G., Leontie L., Şoldea L. C., (1995), Electrical characteristics of some derivatives of p-aminobenzoic acid in thin films, *Progress in Organic Coatings*, **26**, 53-61.
- Turbiez M., Frere P., Allain M., Videlot C., Ackermann J., Roncali J., (2005), Design of organic semiconductors:

tuning the electronic properties of  $\pi$ -conjugated oligothiophenes with the 3,4-ethylenedioxythiophene (EDOT) building block, *Chemistry-A European Journal*, **11**, 3742-3752.

Ueno N., Kera S., (2008), Electron spectroscopy of functional organic thin films: Deep insights into valence electronic structure in relation to charge transport property, *Progress in Surface Science*, **83**, 490-557.